



Original articles

Dynamical behavior of an epidemiological model with a demographic Allee effect

Salisu Usaini^{a,*}, Alun L. Lloyd^b, Roumen Anguelov^a, Salisu M. Garba^a^a Department of Mathematics and Applied Mathematics, University of Pretoria, South Africa^b Department of Mathematics, Center for Quantitative Sciences in Biomedicine and Biomathematics Graduate Program, North Carolina State University, Raleigh, NC 27695, USA

Received 6 January 2015; received in revised form 9 April 2016

Available online 16 June 2016

Abstract

As the Allee effect refers to small density or population size, it cannot be deduced whether or not the Allee mechanisms responsible for an Allee effect at low population density or size will affect the dynamics of a population at high density or size as well. We show using susceptible–exposed–infectious (SEI) model that such mechanisms combined with disease pathogenicity have a detrimental impact on the dynamics of a population at high population level. In fact, the eventual outcome could be an inevitable population crash to extinction. The tipping point marking the unanticipated population collapse at high population level is mathematically associated with a saddle–node bifurcation. The essential mechanism of this scenario is the simultaneous population size depression and the increase of the extinction threshold owing to disease virulence and the Allee effect. Using numerical continuation software MatCont another saddle–node bifurcation is detected, which results in the re-emergence of two non-trivial equilibria since highly pathogenic species cause their own extinction but not that of their host.

© 2016 International Association for Mathematics and Computers in Simulation (IMACS). Published by Elsevier B.V. All rights reserved.

Keywords: Allee effect; Threshold; Extinction; Saddle–node bifurcation

1. Introduction

Single species models with a demographic Allee effect are widely studied by numerous authors (see the review in [11] and the references therein). Density-dependent effects which may either be positive or negative can play an important role in the population dynamics of species by modifying their population *per capita* growth rates. Negative density-dependence acts through various forms of intraspecific competition and prevents a population from growing without bound. On the other hand, at low population density, positive density-dependence is possible through mate availability and cooperative strategies [9,10,15]. The Allee effect has weak and strong forms depending on the

* Correspondence to: Department of Mathematics, Kano University of Science and Technology, Wudil, P.M.B. 3244, Nigeria.

E-mail addresses: kunyasco@yahoo.com (S. Usaini), alun_lloyd@ncsu.edu (A.L. Lloyd), roumen.anguelov@up.ac.za (R. Anguelov), salisu.garba@up.ac.za (S.M. Garba).

strengths of the positive and negative density-dependence [3]. A population exhibits a strong Allee effect if the growth rate is negative at low population size or density. This population size or density is commonly known as the Allee effect threshold below which species collapses to extinction. When the population growth rate is positive at low population size or density, the Allee effect is said to be weak. For the weak Allee effect no threshold of the population size or density exists.

In recent years, a number of authors reported that models with an Allee effect in the host demographics exhibit complex dynamics such as periodic oscillation, multiple stable steady states, and a series of bifurcations. Such bifurcations include sub- and super-critical bifurcations, Bogdanov–Takens bifurcation etc. (see for instance, [7,24,31]). In a similar note, another type of bifurcation called a *backward bifurcation* has been studied in various disease transmission models [14,16,20,21,26–28]. This phenomenon of backward bifurcation involves the existence of a transcritical bifurcation and a saddle–node bifurcation. The occurrence of this phenomenon makes disease eradication more difficult as a stable endemic equilibrium also exists when the basic reproduction number is below unity. We refer the reader to [4] for the detailed description of the backward bifurcation.

The model developed by Hilker [23] in the last decade seems to be the first account of the presence of a bifurcation behavior similar to a backward bifurcation in a model with a demographic Allee effect. The author explored the differences between bifurcation behaviors in epidemiological models without Allee effect that exhibit backward bifurcations and the epidemiological model with the Allee effect. The underlying difference is that a saddle–node bifurcation occurs in the former models when $\mathcal{R}_0 < 1$, whereas it exists in the model with Allee effect if $\mathcal{R}_0 > 1$ (for details, see [23]). It is highlighted in [23] that another saddle–node bifurcation is possible resulting in the re-emergence of two endemic equilibria since highly pathogenic parasites cause their own extinction but not that of their host.

It is obvious that the definition of an Allee effect does not imply any impact at higher population size or density. However, whether or not Allee mechanisms responsible for an Allee effect at low population size or density affect the dynamics of a population at higher population size or density need further investigation.

The main purpose of this study is to investigate the combined impact of Allee effect and infectious disease at higher population levels and to determine which species are more vulnerable to extinction than others under such a situation. In order to achieve that, we extend the susceptible–infectious (SI) model of Hilker [23] by adding the class of exposed individuals. Further, we consider a more general decomposition of the per capita growth as a difference of the per capita births and the per capita deaths which provides ample opportunity for taking into account a wider spectrum of factors causing the Allee effect. More precisely, the impact of cooperative survival strategies, leading to a concave up mortality function, could not be accounted for in the model in [23] where the mortality function is linear. The impact of these factors is adequately represented in the model of this paper via a three parameter decomposition of the growth function.

In addition to the existing similar results in the literature [23], this paper reports that some species are more prone to decline and undergo extinction at higher population size than others, in relation to the effect of density dependence and incubation period of the disease. This is due to adverse conditions caused by the larger population from the Allee effect size and the increase of the effective extinction threshold owing to disease pathogenicity. The extinction scenario is mathematically associated with a saddle–node bifurcation, in which the solution of the system is suddenly lost by disappearance of the two endemic stationary states. As a consequence the system is rendered monostable with extinction as an eventual outcome.

The organization of the paper is as follows: Section 2 presents the model framework. The model is analyzed for its basic properties in Section 3. In Section 4, the existence and stability of equilibria are investigated. In Section 5, bifurcation behavior of the model is considered.

2. Model formulation

Let N be the host total population size at time t . This population is subdivided into three disjoint compartments of individuals that are susceptible ($S(t)$), exposed (latent) ($E(t)$) and infectious ($I(t)$), so that $N(t) = S(t) + E(t) + I(t)$. The respective transfer rates are given in the flow diagram depicted in Fig. 1.

We assume that the force of infection is given by standard incidence (frequency-dependent transmission) and there is no vertical transmission. The dynamics obey the following system of ordinary differential

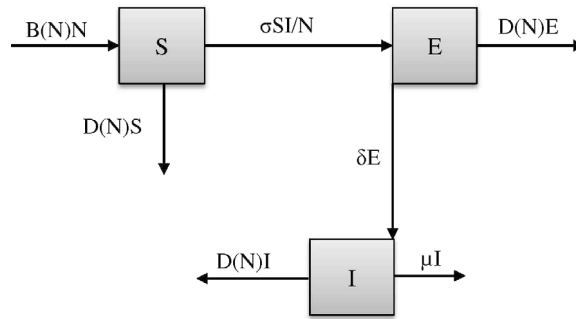


Fig. 1. Flowchart of model (1).

equations:

$$\begin{aligned}
 \frac{dS}{dt} &= B(N)N - \sigma \frac{SI}{N} - D(N)S, \\
 \frac{dE}{dt} &= \sigma \frac{SI}{N} - [\delta + D(N)]E, \\
 \frac{dI}{dt} &= \delta E - [\mu + D(N)]I, \\
 \frac{dN}{dt} &= G(N)N - \mu I,
 \end{aligned} \tag{1}$$

where the parameter σ is the effective contact rate, δ is the rate at which exposed individuals become infected and infected individuals suffer additional disease induced mortality at a rate μ . The density-dependent birth and death rate functions $B(N)$ and $D(N)$, respectively, are obtained by splitting a *per capita* growth rate, $G(N)$ in which a strong Allee effect is manifested. More precisely, we assume that $G(N) = B(N) - D(N)$ satisfies the following assumptions.

- (A1) $G(N)$ is increasing on the interval $[0, N_{\max}]$ and decreasing for $N > N_{\max}$ so that G has a unique maximum at N_{\max} ,
- (A2) The equation $G(N) = 0$ has two positive roots K_- and K_+ , such that $0 < K_- < N_{\max} < K_+ < M$, where M is the upper bound of the domain of system (1).

From (A1) and (A2) we obtain that $G(N) > 0$ for $N \in (K_-, K_+)$. Therefore (denoting $' = \frac{d}{dN}$)

- (B1) $B(N) > D(N)$ for $N \in (K_-, K_+)$ with $B(K_+) = D(K_+)$ and $B'(K_+) < D'(K_+)$,
- (B2) $B(N) < D(N)$ for $N \in [0, K_-) \cup (K_+, M)$ with $B(K_-) = D(K_-)$ and $B'(K_-) > D'(K_-)$.

In order to make system (1) non-dimensional, we re-scale the variables of the model (1) by

$$s = \frac{S}{N}, \quad e = \frac{E}{N}, \quad i = \frac{I}{N} \quad \text{and} \quad p = \frac{N}{K_+}$$

so that $s + e + i = 1$ and system (1) becomes

$$\begin{aligned}
 \frac{dp}{dt} &= [g(p) - \mu i]p, \\
 \frac{de}{dt} &= \sigma(1 - i)i - [\delta + b(p) + (\sigma - \mu)i]e, \\
 \frac{di}{dt} &= \delta e - [b(p) + \mu(1 - i)]i,
 \end{aligned} \tag{2}$$

where $g(p), b(p)$ are the dimensionless forms of $G(N)$ and $B(N)$, respectively. More precisely, we have $g(p) = G(pK_+)$ and $b(p) = B(pK_+)$. Then the assumptions (A1) and (A2) imply that on $[0, m], m = \frac{M}{K_+}$, $g(p)$ has two positive roots $u = \frac{K_-}{K_+} \in (0, 1)$ and 1 with a unique maximum between the roots.

3. Basic properties of the model

3.1. Model (2) as a dynamical system

Theorem 1. *The system of differential equations (2) defines a dynamical system on the region*

$$\Omega = \{(p, e, i) \in \mathbb{R}_+^3 : 0 \leq p \leq m, 0 \leq e, i, e + i \leq 1\}.$$

Proof. We need to show that all solutions of (2) initiated in Ω do not leave Ω . Then the statement of the theorem follows from the boundedness of Ω , see [30, Theorem 2.1.5]. The region Ω is a triangular prism in the (p, e, i) -space. It is easy to see that the line $e = i = 0$ and the plane $p = 0$ are invariant sets of system (2). Then it remains to show that the vector field defined via the right hand side of (2) is directed inwards at the remaining part of the boundary of Ω . Since this involves standard arguments we will show it only for one face of the prism Ω , namely $e + i = 1, e, i \geq 0, 0 \leq p \leq m$. The outward normal vector to this face is $(0, 1, 1)$. Therefore it is sufficient to show that $\frac{de}{dt} + \frac{di}{dt} < 0$. We have

$$\frac{de}{dt} + \frac{di}{dt} = (\sigma - \mu)[1 - (e + i)]i - b(p)(e + i) = -b(p) < 0,$$

which completes the proof. ■

3.2. Threshold quantities

There are two well known ways of a disease control for disease transmission models with varying population size (i.e. a population with increasing or decreasing total size) due to demographic effects [6,5]. The first way requires that the proportion $i(t)$ of infectives goes to zero, whereas the second requirement is that the absolute number $I(t)$ of infectives approaches to zero. These notions of disease elimination were given and discussed in some detail in [5]. Thus, the conditions for the linear stability of disease free equilibria and for the existence and stability of endemic proportion equilibria are required. The pertinent threshold parameters are as follows

$$\mathcal{R} = \mathcal{R}(p) = \frac{\delta\sigma}{[\delta + b(p)][\mu + b(p)]}, \quad (3)$$

from which, we have

$$\mathcal{R}_0 = \mathcal{R}(1), \quad \mathcal{R}_u = \mathcal{R}(u), \quad \text{and} \quad \mathcal{R}_e^* = \mathcal{R}(0),$$

according as the population is at its carrying capacity ($p = 1$), minimum survival level ($p = u$) or extinction state ($p = 0$), respectively.

It is important to note that the demographic functions $b(p)$ and $d(p)$ are equal at the carrying capacity state and Allee threshold state. Thus, the threshold parameters \mathcal{R}_0 and \mathcal{R}_u , are equivalently represented as

$$\mathcal{R}_0 = \frac{\delta\sigma}{[\delta + d(1)][\mu + d(1)]}, \quad \mathcal{R}_u = \frac{\delta\sigma}{[\delta + d(u)][\mu + d(u)]}. \quad (4)$$

It is instructive to remark that the threshold parameters \mathcal{R} and \mathcal{R}_0 represent the usual replacement and reproduction numbers, respectively, that appear in disease transmission models. The distinction between the two threshold quantities can be found in [22].

4. Equilibria and their stability

4.1. Trivial equilibria

In the absence of the disease, model (2) has the following equilibrium points:

- (i) $\mathcal{E}_0 = (0, 0, 0)$: trivial extinction state,
- (ii) $\mathcal{E}_1 = (u, 0, 0)$: Allee threshold state, and
- (iii) $\mathcal{E}_2 = (1, 0, 0)$: carrying capacity state.

Obviously, $\mathcal{R}_0 \leq 1$ if and only if $\delta(\sigma - \mu) - b(1)[\mu + \delta + b(1)] \leq 0$ if $\sigma - \mu \leq 0$. The condition $\sigma - \mu \leq 0$ leads to the extinction of disease $i(t)$ of system (2). Therefore, the disease cannot invade from arbitrarily small introductions into the host population at carrying capacity whenever $\mathcal{R}_0 \leq 1$.

Theorem 2. Model (2) has three disease free equilibria: $\mathcal{E}_0, \mathcal{E}_1$ and \mathcal{E}_2 . The equilibrium \mathcal{E}_0 is a stable node if $\mathcal{R}_e^* < 1$ and is a saddle point if $\mathcal{R}_e^* > 1$. The equilibrium \mathcal{E}_2 is also a stable node if $\mathcal{R}_0 < 1$ and is a saddle point if $\mathcal{R}_0 > 1$. The Allee threshold equilibrium \mathcal{E}_1 is always a saddle point.

Proof. The Jacobian matrix, denoted by $J^*(p, 0, 0)$ evaluated around a disease-free equilibrium $(p, 0, 0)$ of system (2) is given by

$$J_{df}(p, 0, 0) = \begin{pmatrix} g'(p)p + g(p) & 0 & -\mu p \\ 0 & -[\delta + b(p)] & \sigma \\ 0 & \delta & -[\mu + b(p)] \end{pmatrix}.$$

It follows that the matrix $J_{df}(\mathcal{E}_0)$ has eigenvalues $\lambda_1 = b(0) - d(0) < 0$ since $p < u$ and the eigenvalues of the matrix obtained by deleting the first row and column of $J_{df}(\mathcal{E}_0)$, denoted by $J_{df}^*(\mathcal{E}_0)$. Then, the trace and determinant of $J_{df}^*(\mathcal{E}_0)$ are, respectively, given by

$$\text{tr}(J_{df}^*(\mathcal{E}_0)) = -[\mu + \delta + 2b(0)] < 0$$

and

$$\det(J_{df}^*(\mathcal{E}_0)) = [\mu + b(0)][\delta + b(0)] - \delta\sigma \geq 0,$$

since $\mathcal{R}_e^* < 1$ if $\delta\sigma \leq [\mu + b(0)][\delta + b(0)]$ and $\mathcal{R}_e^* > 1$ when $\delta\sigma > [\mu + b(0)][\delta + b(0)]$. Furthermore, the corresponding eigenvalues of $J_{df}^*(\mathcal{E}_0)$ are:

$$\lambda_{2,3} = \frac{1}{2}\{-([\mu + b(0)] + [\delta + b(0)]) \pm \sqrt{([\mu + b(0)] - [\delta + b(0)])^2 + 4\delta\sigma}\},$$

which are distinct real and of either negative sign if $\mathcal{R}_e^* < 1$ or opposite sign when $\mathcal{R}_e^* > 1$. Hence, the trivial extinction state \mathcal{E}_0 is a stable node whenever $\mathcal{R}_e^* < 1$ and a saddle point otherwise.

For $p = 1$ the first eigenvalue of $J_{df}(\mathcal{E}_2)$ is $\lambda_1 = [b'(1) - d'(1)] < 0$ by (B1). Then, by simply replacing $b(0)$ with $b(1)$ in the above arguments for $J_{df}^*(\mathcal{E}_0)$, one can verify that the carrying capacity state \mathcal{E}_2 is also a stable node if $\mathcal{R}_0 < 1$ and a saddle point when $\mathcal{R}_0 > 1$.

Using a similar argument as in the case when $p = 0$ and $p = 1$, the first eigenvalue of $J_{df}(\mathcal{E}_1)$ is $\lambda_1 = [b'(u) - d'(u)]u > 0$ by (B2) and the other two eigenvalues are distinct real and of either negative sign when $\mathcal{R}_0 < 1$ or opposite sign if $\mathcal{R}_0 > 1$. Therefore, the Allee threshold state is always a saddle point. ■

4.2. Semi-trivial and non-trivial equilibria

The steady states of model (2) where at least one of the infected compartments of the model is non-empty are called non-trivial equilibria. These equilibrium points can be obtained by setting the right-hand sides of system (2) to zero and solving the resulting algebraic equations. Thus, setting the right-hand sides of model (2) to zero, we obtain

$$p = 0 \text{ or } i = \frac{g(p)}{\mu}, \quad e = \frac{\sigma(1-i)i}{\delta + b(p) + (\sigma - \mu)i}, \quad e = \frac{\mu(1-i) + b(p)}{\delta}i, \tag{5}$$

thus i satisfies $f(i) = 0$, where

$$f(i) = \mu(\sigma - \mu)i^2 - \{(\sigma - \mu)[\mu + \delta + b(p)] - \mu b(p)\}i + \delta\sigma - [\mu + b(p)][\delta + b(p)]. \tag{6}$$

For the non-trivial equilibria to be biologically feasible, we require that $g(p) > 0$ since $g(p) < 0$ for $p \in (0, u) \cup (1, m)$ by (B2) and $\delta + b(p) + (\sigma - \mu)i > 0$. Obviously, the second condition holds when $\sigma > \mu$ and so, in the following analysis we assume that $\sigma > \mu$. This condition also applies to the semi-trivial equilibrium. Conditions for the existence and biological feasibility of the semi-trivial and non-trivial equilibria are presented in the following lemma.

Lemma 1. Model (2) has

- (i) a semi-trivial equilibrium $\mathcal{E}_s = (0, e_s, i_s)$ if $\mathcal{R}_e^* > 1$,
- (ii) non-trivial equilibrium if $\mathcal{R}_u > 1$ for a fixed p .

Proof. (i) Let $\mathcal{R}_e^* > 1 \Rightarrow (\sigma - \mu) > \frac{\mu b(0)}{\delta}$ (i.e. $(\sigma - \mu) > 0$). Then it follows from (6) that $f(0) > 0$, and $f(1) = -\{2\mu + [(\sigma - \mu) + \delta + b(0)]b(0)\} < 0$. Therefore, $f(i)$ has a root $i_1 \in (0, 1)$, and a second root $i_2 > 1$. This implies from the last equation of (5) that $e_s \geq 0$. Furthermore, setting the right-hand sides of the second and third equations of (2) to zero, adding and simplifying gives

$$[\sigma + b(0)]e_s = \{[\sigma - \mu](1 - i_s) + \mu e_s\}i_s. \quad (7)$$

The left-hand side of (7) is positive and $\sigma > \mu$. Hence, $i_s \in (0, 1)$ and this completes the existence proof.

(ii) Following similar argument as in Case (i), we have from the last equation of (5) that $e^* \geq 0$. Also for a fixed p , say p^* , we obtain from the second and third equations of (2) that

$$[\sigma + b(p^*)]e^* = \{[\sigma - \mu](1 - i^*) + \mu e^*\}i^*. \quad (8)$$

Then, $\mathcal{R}_u > 1$ implies that $\sigma > \mu$ so that $i^* \in (0, 1)$ since the left hand side of (8) is positive. Hence the proof. ■

Remark 1. The steady state solutions (p^*, i^*) satisfy the following inequality (noting that $f(0) > 0$ and $f(1) < 0$)

$$i^* < \frac{[\sigma - \mu][\mu + \delta + b(p^*)] - \mu b(p^*)}{2\mu[\sigma - \mu]}.$$

The above results (Lemma 1) assert that the semi-trivial equilibrium exists and is biologically feasible if $\mathcal{R}_e^* > 1$, while the non-trivial equilibrium exists and is biologically feasible if $\mathcal{R}_u > 1$ (since the disease cannot invade a population at the edge of extinction owing to the strong Allee effect if $\mathcal{R}_u \leq 1$).

4.2.1. Semi-trivial equilibrium

A semi-trivial equilibrium is a steady state of the model (2) where the disease exterminates the host population. Let $\mathcal{E}_s = (p_s, e_s, i_s)$ be such an equilibrium point of system (2). Then from Eqs. (5) and (6), we have

$$p_s = 0, \quad e_s = \frac{\mu(1 - i_s) + b(0)}{\delta}i_s,$$

and i_s solves

$$\frac{\delta\sigma(1 - i_s)}{[\mu(1 - i_s) + b(0)][\delta + b(0) + (\sigma - \mu)i_s]} = 1. \quad (9)$$

Theorem 3. The semi-trivial extinction state (\mathcal{E}_s) of model (2) is locally asymptotically stable if $\mathcal{R}_e^* > 1$ and unstable otherwise.

Proof. The proof is by linearization as in the proof of Theorem 2.

4.2.2. Non-trivial equilibria

It follows from Lemma 1 that if $\mathcal{R}_0 > 1$, then for some fixed p model (2) has non-trivial equilibrium. Therefore, for p^* at endemic state, we have from (5) that

$$e^* = \frac{\mu(1 - i^*) + b(p^*)}{\delta}i^*, \quad i^* = \frac{g(p^*)}{\mu}, \quad (10)$$

and i^* solves

$$\frac{\sigma\delta(1 - i^*)}{[\mu(1 - i^*) + b(p^*)][\delta + (\sigma - \mu)i^* + b(p^*)]} = 1. \quad (11)$$

Note that (11) is obtained by equating the last two expressions for e in (5).

Furthermore, the endemic equilibria of system (2) correspond to the roots of the following equation in $(u, 1)$

$$\Psi(p) = [\mu + d(p)]\{\mu[\delta + b(p)] + (\sigma - \mu)g(p)\} + \sigma\delta[g(p) - \mu], \tag{12}$$

with

$$e = \frac{\mu(1 - i) + b(p)}{\delta}i, \quad i = \frac{g(p)}{\mu}.$$

To investigate the possible number of positive interior equilibria via phase plane illustration, Eq. (12) with $g(p) = \mu i$ is rewritten in the form

$$i = \frac{\sigma\delta - [\mu + d(p)][\delta + d(p)]}{\sigma[\mu + \delta + d(p)]}. \tag{13}$$

Then, we call (13) the infected nullcline or simply i -nullcline. Furthermore, we denote by $\Phi_1(p)$ and $\Phi_2(p)$ the host and infected nullclines, respectively. Therefore, endemic equilibria can be found as the intersections of the i -nullcline in (13) and the p -nullcline $i = g(p)/\mu$. In order to demonstrate this, we consider the following *per capita* net growth rate used by Hilker [24].

$$G(N) = a(K_+ - N)(N - K_-), \quad 0 < K_- \ll K_+, \tag{14}$$

where K_- is the minimum viable density through which the strong Allee effect is manifested. The parameter K_+ is the carrying capacity and the coefficient $a > 0$ adjusts the maximum *per capita* growth rate.

To model the factors responsible for the Allee effects we decompose the *per capita* growth rate function in (14) as $G(N) = B(N) - D(N)$. Such a decomposition was explained in detail and the demographic rate functions $B(N)$ and $D(N)$ were represented in [32] as follows:

$$\begin{aligned} B(N) &= a\{-(1 - \alpha)N^2 + [K_+ + (1 - \beta)K_-]N + K_+\Gamma\}, \\ D(N) &= a(\alpha N^2 - \beta K_-N + K_+K_- + K_+\Gamma), \end{aligned} \tag{15}$$

where the parameters $\alpha \in [0, 1)$, β and $\Gamma \geq 0$ determine the decomposition of the growth rate function $G(N)$ as a difference of the birth rate $B(N)$ and the death rate $D(N)$ similar to the approach in [24]. Moreover, β and Γ as in [24], determine the effect of density dependence and independence in both mortality and fertility rate functions, respectively. The demographic functions (15) generalize the model in [24] by providing decomposition of the quadratic term in $G(N)$ and not only of its linear part. The basic requirement that both the demographic rate functions need to be biologically meaningful places some constraints on the values of β and Γ . One can easily see that under the restriction

$$\beta \leq \min\{1, 2\sqrt{2\alpha}\} \tag{16}$$

both functions are positive on the interval $[0, M]$ where $M = \frac{(1-\beta)K_-+K_+}{1-\alpha}$. Detailed explanation of these demographic rate functions can be found in [32].

The motivation behind the choice of the birth rate function $B(N)$ is the improved access to abundant resources, e.g. via cooperative strategies. The function $D(N)$ takes into account Allee effect factors which decrease mortality as population size increases. These include joint defence, lower individual exposure to predation, cooperation in raising the young, etc. Representing $D(N)$ as a quadratic function ($\alpha > 0$) is essential for considering these factors. Indeed, due to the quadratic term in $D(N)$, at low population levels $D(N)$ is either increasing at a slower rate ($\beta \leq 0$) or is decreasing ($\beta > 0$). More precisely, the strength of the impact of cooperative survival strategies on mortality at low population level is represented via the gradient of D in a small positive neighborhood of 0. It can be conveniently measured by the parameter β . Indeed, the gradient of $D(N)$ at 0, that is $D'(0) = -a\beta K_-$, linearly depends on β . Small value of $D'(0)$ or equivalently large value of β indicates strong impact. We can also observe that when β is large negative the graph of the function $D(N)$ is close to a straight line on $[0, M]$. As β increases the impact becomes more pronounced. If $\beta > 0$ then $D(N)$ is decreasing on $[0, \frac{\beta K_-}{2\alpha}]$, thus representing a strong impact of cooperative survival strategies. Obligate cooperative species would be in this category. If $\alpha = 0$ the model is similar to the model in [24]. In this particular case, the restriction (16) implies $\beta \leq 0$. Hence, the mortality rate increases with a constant gradient for all population sizes.

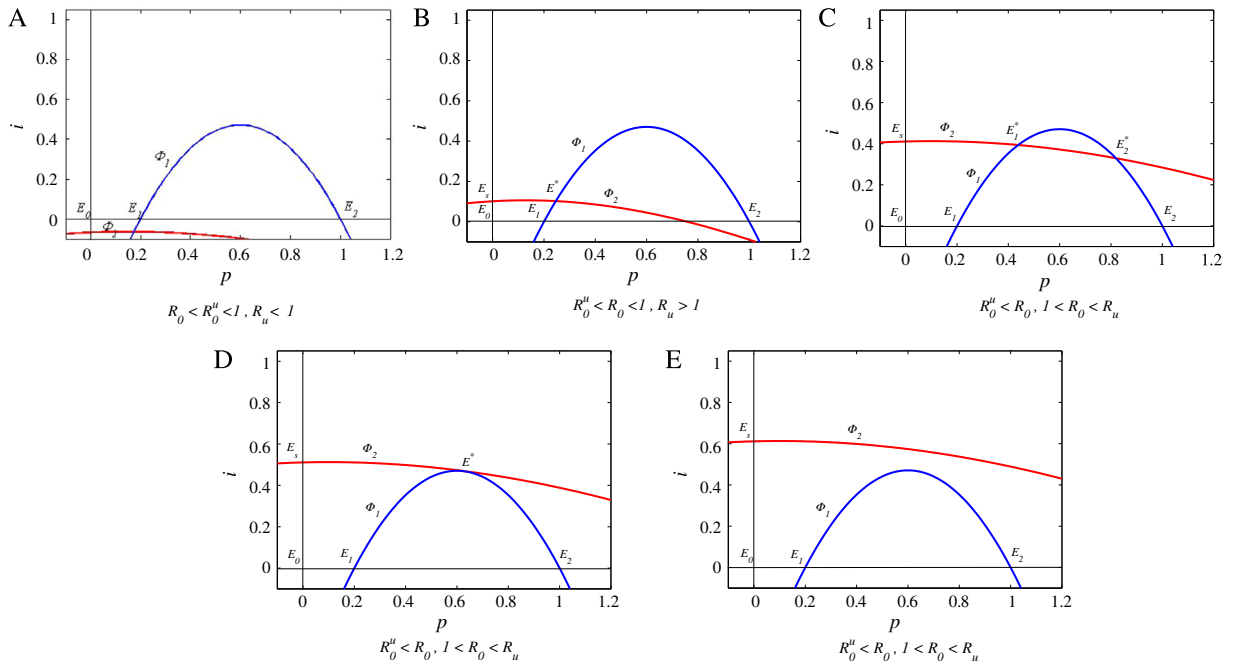


Fig. 2. Phase plane illustrations with nullclines and endemic states of model (2) with (17). Parameter values used for all curves are $k = 0.5, u = 0.2, \mu = 0.17$ and other parameters are stated in each part. (A) shows that there is no endemic state in the interval $(u, 1)$, where the curves are drawn with $\alpha = 0.2, \beta = 0.3, \gamma = 0.01, \sigma = 0.7$ and $\delta = 0.06$; (B) shows one endemic state for $\alpha = 0.35, \beta = 0.45, \gamma = 0.002, \sigma = 0.95$ and $\delta = 0.1$; (C) shows two endemic states with $\alpha = 0.2, \beta = 0.2, \gamma = 0.05, \sigma = 0.995$ and $\delta = 0.55$; (D) shows that the two equilibria in (B) coincide in one when $\gamma = 0.011, \delta = 0.78$; (E) indicates that the two endemic states disappear by saddle–node bifurcation for $\gamma = 0.0001, \sigma = 1.1$ and $\delta = 0.78$.

Death and birth are fundamental mechanisms used by populations to combat disease. This is particularly true when there is no vertical transmission as in the case of model (1). Therefore, the birth rate and death rate functions have a significant impact on the disease dynamics. The more general form of these functions (15) not only extends the model in [24] by considering a wider spectrum of the Allee effect factors, but it also provides a parametrization of model (1) which more adequately captures the epidemiological impact of the Allee effect. Indeed, we show in the sequel that some biologically realistic asymptotic states are only possible when $\alpha > 0$ and $\beta > 0$.

The dimensionless forms of the demographic functions in (15) as explained below Eq. (2) are as follows:

$$\begin{aligned}
 b(p) &= k[-(1 - \alpha)p^2 + (1 + u - \beta u)p + \gamma], \\
 d(p) &= k(\alpha p^2 - \beta u p + u + \gamma),
 \end{aligned}
 \tag{17}$$

where $\gamma = \frac{\Gamma}{K_+} \geq 0$ so that both the birth and the death rate functions are positive in the interval $[0, m]$ for $m = \frac{M}{K_+} = \frac{1+u(1-\beta)}{1-\alpha}$. The non-trivial equilibria of model (2) with (17) are then depicted in Fig. 2.

It follows from the algebraic forms of host and infected nullclines that model (2) with (17) can have two biologically feasible endemic equilibria as shown in Fig. 2. We denote such equilibria by $\mathcal{E}_1^* = (p_1^*, e_1^*, i_1^*)$ and $\mathcal{E}_2^* = (p_2^*, e_2^*, i_2^*)$, respectively, where $p_1^* < p_2^*$.

Theorem 4. *The endemic equilibrium, \mathcal{E}_2^* with a large population size when it exists is locally asymptotically stable in the interior of the domain, Ω if $\mathcal{R}_0 > 1$. While the endemic equilibrium, \mathcal{E}_1^* with low population size, if it exists is always unstable.*

Proof. Linearizing system (2) around an endemic equilibrium \mathcal{E}^* , gives the following Jacobian matrix

$$J^* = \begin{pmatrix} [b'(p^*) - d'(p^*)]p^* & 0 & -\mu p^* \\ -b'(p^*)e^* & -\kappa & \sigma(1 - 2i^*) - (\sigma - \mu)e^* \\ -b'(p^*)i^* & \delta & -b(p^*) - \mu(1 - 2i^*) \end{pmatrix}$$

where $\kappa = [\delta + b(p^*) + (\sigma - \mu)i^*]$. The characteristic equation of the matrix J^* simplified using Eq. (11) and e^*, i^* in (10), is

$$\lambda^3 + a_2\lambda^2 + a_1\lambda + a_0 = 0,$$

where

$$\begin{aligned} a_2 &= -[b'(p^*) - d'(p^*)]p^* + (\sigma - \mu)i^* + \mu + \delta + 2d(p^*), \\ a_1 &= p^*d'(p^*)[(\sigma - \mu)i^* + \mu + \delta + 2d(p^*)] - p^*b'(p^*)[\sigma i^* + \mu + \delta + 2d(p^*)] \\ &\quad + [(\sigma - \mu)(\mu + \delta + b(p^*) - \mu i^*) - \mu b(p^*)]i^*, \\ a_0 &= p^*i^*\{d'(p^*)[(\sigma - \mu)(\mu + \delta + b(p^*) - \mu i^*) - \mu b(p^*)] - b'\sigma(\mu + \delta + b(p^*))\}. \end{aligned}$$

It follows from the condition $\mathcal{R}_0 > 1$ and Remark 1 that $a_i > 0$ for $i = 0, 1, 2$ if $p^* = p_2^*$. Hence, by the Routh–Hurwitz criteria [29], \mathcal{E}_2^* is locally asymptotically stable if and only if $a_1a_2 > a_0$. To show that $a_1a_2 > a_0$, write $a_i = x_i v + y_i w + z_i$ where $v = -p_2^*b'(p_2^*)$ and $w = p_2^*d'(p_2^*)$ for all $x_i, y_i, z_i, v, w \geq 0$. Then the condition for local stability is

$$\begin{aligned} a_1a_2 - a_0 &= (x_1v + y_1w + z_1)(x_2v + y_2w + z_2) - (x_0v + y_0w + z_0), \\ &= x_1x_2v^2 + y_1y_2w^2 + (x_1y_2 + y_1x_2)vw + (x_1z_2 + z_1x_2 - x_0)v \\ &\quad + (y_1z_2 + x_1y_2 - y_0)w + z_1z_2 - z_0 > 0. \end{aligned}$$

One can easily see that $x_1z_2 > x_0, y_1z_2 > y_0$ and $z_1z_2 - z_0 = z_1z_2 > 0$ so that $a_1a_2 - a_0 > 0$. Therefore, \mathcal{E}_2^* is locally asymptotically stable.

For $p^* = p_1^*$ the stability condition $a_1a_2 > a_0$ is not satisfied because \mathcal{E}_1^* establishes an extinction basin above the Allee threshold and, so \mathcal{E}_1^* is always unstable. ■

Further, rewriting $\Psi(p)$ as defined in (12) in the form

$$\Psi(p) = g(p) - \mu \frac{\sigma\delta - [\mu + d(p)][\delta + d(p)]}{\sigma[\mu + \delta + d(p)]}, \tag{18}$$

we obtain

$$\begin{aligned} \Psi(u) &= -\frac{\mu}{\sigma[\mu + d(u)][\delta + d(u)][\mu + \delta + d(u)]}[\mathcal{R}_u - 1], \\ \Psi(1) &= -\frac{\mu}{\sigma[\mu + d(1)][\delta + d(1)][\mu + \delta + d(1)]}[\mathcal{R}_0 - 1]. \end{aligned} \tag{19}$$

It follows that $\Psi(u) = 0 \Leftrightarrow \mathcal{R}_u = 1$ and $\Psi(1) = 0 \Leftrightarrow \mathcal{R}_0 = 1$. Using these relations, we define an invasion threshold, denoted by \mathcal{R}_0^u as follows.

$$\mathcal{R}_0^u = \frac{\mathcal{R}_0}{\mathcal{R}_u} = \frac{[\mu + d(u)][\delta + d(u)]}{[\mu + d(1)][\delta + d(1)]}.$$

Thus, we establish the following results.

Theorem 5. Model (2) with (17) has:

- (i) no non-trivial equilibrium if $\mathcal{R}_0 \leq 1$ and $\mathcal{R}_0 \leq \mathcal{R}_0^u$ (i.e. $\mathcal{R}_u \leq 1$),
- (ii) a unique endemic equilibrium $\mathcal{E}^* = (p^*, e^*, i^*)$ if $\mathcal{R}_0 \leq 1 < \mathcal{R}_u$. This equilibrium is always unstable, and, in the presence of disease, is the effective eradication threshold since the extinction basin is increased beyond the Allee threshold in such a case.

Theorem 5 shows that if $\mathcal{R}_0 \leq 1$ the only stable equilibria are the disease free carrying capacity and an extinction state \mathcal{E}_0 or \mathcal{E}_s . In case (i), the system does not have any endemic equilibria when in addition we have $\mathcal{R}_u \leq 1$. While in case (ii), when $\mathcal{R}_u > 1$, it has an unstable endemic equilibrium. This does not change the bistability of the system, but has a significant impact on the shape of the trajectories. For example, we may have an epidemic for initial populations in the interval $(u, 1)$. The existence of the equilibrium \mathcal{E}^* further shows explicitly that population extinction is possible even when the initial population is above the Allee threshold u . Let us note that case (ii) of the theorem is only possible

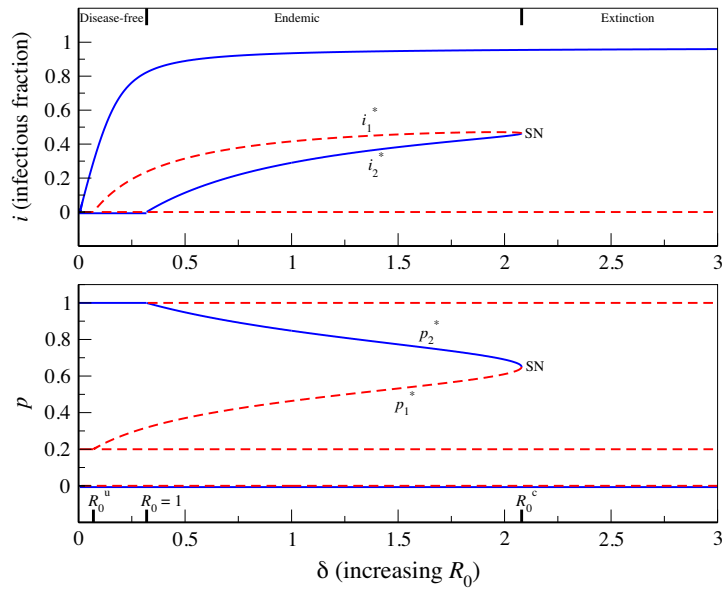


Fig. 3. Bifurcation diagrams for varying δ (increasing \mathcal{R}_0), showing the biologically feasible equilibria. Solid (dashed) lines represent stable (unstable) equilibria and *SN* indicates a saddle–node bifurcation above which the population collapse. Parameter values used are $k = 0.5, u = 0.2, \mu = 0.17, \alpha = 0.2, \gamma = 0.05$ and $\sigma = 1$.

when $\alpha > 0$ and $\beta > 0$. Indeed, using (4), the inequality $\mathcal{R}_0 < \mathcal{R}_u$ implies that $d(u) > d(1)$. Then from the properties of $d(p)$ in (16) as a quadratic function of p it follows that α and β are positive.

5. Bifurcation analysis of the model with quadratic demographic functions

It is evident that, when an epidemiological model admits multiple non-trivial equilibria, the model usually exhibits complex dynamical behavior such as backward bifurcation and forward hysteresis [18,19,21,25]. However, the existence of two non-trivial and biologically feasible steady states when $\mathcal{R}_0 > 1$ as shown in Fig. 2(C) indicates that model (2) with (17) will have complex dynamics.

Keeping all the parameters fixed other than the latency parameter δ , we take δ as the bifurcation parameter. It should be noted that as bifurcation parameters, δ and \mathcal{R}_0 can be considered essentially equivalent. More precisely, \mathcal{R}_0 can be regarded as a function of δ so that \mathcal{R}_0 is varied by varying the latency parameter δ . We denote by δ^c the value of δ at which the two endemic states coincide as in Fig. 2(D) with corresponding critical threshold parameter $\mathcal{R}_0^c = \mathcal{R}_0(\delta^c)$. However, in the rest of this section we will discuss the dynamical behavior of model (2) with (17) in terms of \mathcal{R}_0 . In a similar note we can take \mathcal{R}_0 as a function of either β or the transmissibility σ to obtain bifurcation results similar to those for δ as in Fig. 6 in Appendix A and those presented in [23], respectively. The bifurcation diagrams with σ as bifurcation parameter are not shown here as they are qualitatively equivalent to those presented by Hilker in [23] and so, we refer the reader to the paper of Hilker [23].

Using the numerical continuation software ‘MatCont’ (a graphical MATLAB software package for the interactive numerical study of dynamical systems, which allows one to compute curves of equilibria, limit points, Hopf points, limit cycles, period doubling bifurcation points of limit cycles, and fold bifurcation points of limit cycles) [12], we show in Fig. 3 how the total population p and prevalence i change with varying the threshold parameter \mathcal{R}_0 . If $\mathcal{R}_0 < 1$, the disease cannot invade the population at carrying capacity. If $\mathcal{R}_0 > 1$, however, the disease-free equilibrium \mathcal{E}_2 loses stability, resulting in the emergence of a locally stable endemic equilibrium \mathcal{E}_2^* by transcritical bifurcation. This endemic equilibrium coexists with the unstable equilibrium \mathcal{E}_1^* that already arises when $\mathcal{R}_0 > \mathcal{R}_0^u$. The two endemic equilibria coalesce and disappear by a saddle–node (SN) bifurcation at $\mathcal{R}_0 = \mathcal{R}_0^c$. Hence, the population goes extinct.

Furthermore, the sub-threshold \mathcal{R}_0^c is a tipping point for an unanticipated population collapse. Therefore, the system is rendered monostable whenever $\mathcal{R}_0 > \mathcal{R}_0^c$ with trivial extinction state \mathcal{E}_0 being the only global attractor. If $\mathcal{R}_0 < \mathcal{R}_0^c$, the system is bistable with one of the attractors being either an extinction state, \mathcal{E}_0 if $\mathcal{R}_e^* < 1$ or semitrivial extinction state (\mathcal{E}_s) when $\mathcal{R}_e^* > 1$. The other attractor is either \mathcal{E}_2 if $\mathcal{R}_0 < 1$ or \mathcal{E}_2^* when $\mathcal{R}_0 > 1$.

One can observe from Fig. 7 in Appendix B that the tipping point \mathcal{R}_0^c for the abrupt population collapse increases with increasing and decreasing values of β and δ , respectively. Therefore, the high extinction risk from high population levels depends on the incubation period (i.e., the value of δ) and the strength of the impact of cooperative survival strategies which is measured by the parameter β . For example, if $\delta = 0.3$, the incubation period is approximately 3 units, then $\beta = 0.3$ for the abrupt population collapse. However, when $\delta = 4$, the parameter $\beta = -13$ so that the incubation period is 0.25 units which is small. This simply shows that, if disease incubation period is small and the strength of the impact of cooperative survival strategies is less, then non-obligate cooperative species are more vulnerable to decline and extinction at high population level. While obligate cooperators have high extinction risk under such a situation when the incubation period is large and the impact of cooperative survival strategies is strong. The essential mechanism behind this scenario is the simultaneous population size depression and the increase of the extinction threshold due to disease virulence and the Allee effect.

It is worth mentioning here that all the results of model (2) with (17) hold true for its special cases. These are the cases when the demographic function $d(p)$ in (17) becomes linear and constant for $\alpha = 0$ and $\alpha = \beta = 0$, respectively. For the first case, if $\beta = -1/ku$, then the demographic functions in (17) are similar to those in [23]. In this case, we have an extended version of the model of Hilker [23]. Moreover, the bifurcation results here are similar to those in [23], showing the robustness of the outcomes of an interaction of Allee effects and infectious disease, which makes the predictability of such systems easier. However, the novelty of the presented model is the dynamic parameter β that makes the model more general and determines which species are more prone than others to decline and extinction depending on the latency parameter δ . Determining the parameter β , plays a relevant role in conservation biology for guiding management actions, as it would allow biologists to predict the vulnerability of species to extinction even before they decline, thereby improving the species' chances of survival.

It is to be noted that the threshold \mathcal{R}_0 can also be altered by varying the pathogenicity μ . In fact, an increase in \mathcal{R}_0 corresponds to a decrease in μ . In such situations, another critical threshold parameter denoted by \mathcal{R}_0^{c2} such that $\mathcal{R}_0^{c2} > \mathcal{R}_0^{c1}$ also exists for which a second saddle–node bifurcation occurs. This scenario gives rise to two non-trivial equilibria again after the extinction regime at $\mathcal{R}_0 = \mathcal{R}_0^{c2}$. The bifurcation diagrams that reveal the second saddle–node bifurcation, which are obtained using the numerical continuation software MatCont [12] are depicted in Fig. 4.

As was reported in [1,2], the maximum degree of depression of the host population equilibrium (here leading to extinction) is achieved by a disease with intermediate pathogenicity (i.e. moderate to large \mathcal{R}_0). When the disease pathogenicity is too small, i.e. too high a \mathcal{R}_0 , the disease has little detrimental effect on the host. In such a case, the host persists at endemic state with large population size ($\mathcal{R}_0 > \mathcal{R}_0^{c2}$). In contrast, if the level of disease pathogenicity is too high, i.e. too small a \mathcal{R}_0 , the increased mortality of infected individuals will either prevents effective disease transmission ($1 < \mathcal{R}_0 < \mathcal{R}_0^{c1}$) or even leads to the deletion of infections from the host population ($\mathcal{R}_0 < 1$).

It is observed that the threshold quantities of the model define a nonlinear relationship between δ and μ and a linear relationship between σ and μ as in [23], while the saddle–node bifurcation conditions define a nonlinear relationship. Thus, the summary of the model behavior in the two-parameter space (μ, σ) is depicted in Fig. 5. Therefore, the dynamical consequences of model (2) with (17) can be characterized in relation to disease-related parameters σ and μ . As highlighted in [23], fixing the pathogenicity μ corresponding to a saddle–node bifurcation scenario and traversing vertically through Fig. 4 by altering σ reveals that the saddle–node bifurcation curve can be crossed only once. Similarly, if transmissibility σ (noting the critical value of σ at the turning point of the saddle–node bifurcation curve) is fixed and Fig. 4 is traversed horizontally by varying μ , the saddle–node bifurcation curve can be crossed twice (revealing the existence of two saddle–node bifurcations). The mathematical implication of these numerical observations is that both nullclines depend on μ , but only one nullcline depends on σ .

6. Discussion and conclusions

The Allee effect refers to a reduction of individuals fitness, which leads to a decreasing population *per capita* growth rate in low densities or small population sizes. However, there is increasing evidence for the impact of an Allee effect at high densities or large population sizes [13,23]. The model considered in [13] suggests that a small

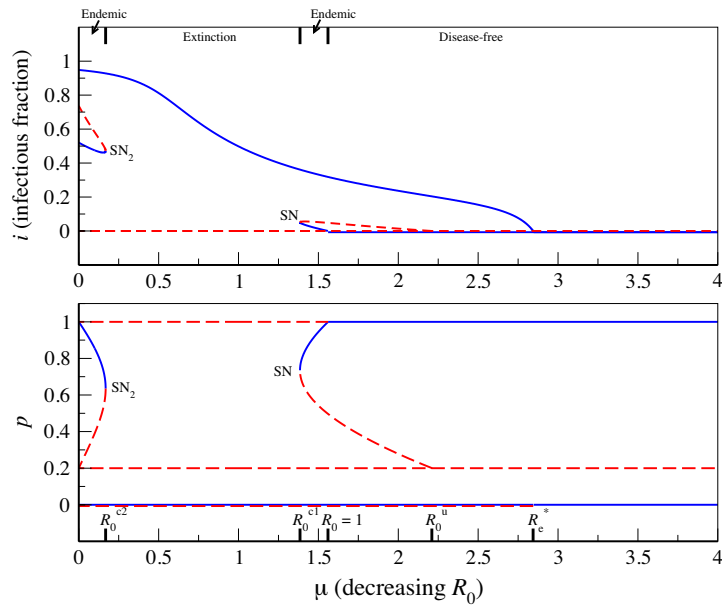


Fig. 4. Bifurcation diagrams that reveal a second saddle–node bifurcation by changing disease pathogenicity μ (decreasing \mathcal{R}_0). The locations of the associated threshold parameters are indicated on μ -axis. The extinction equilibria \mathcal{E}_0 and \mathcal{E}_s exchange stability at $\mathcal{R}_e^* = 1$ by transcritical bifurcation. Solid (dashed) lines represent stable (unstable) equilibria and SN indicates a saddle–node bifurcation above which the population collapse. While SN_2 shows a second saddle–node bifurcation for the re-emergence of two endemic equilibria. Parameter values used are $k = 0.5, u = 0.2, \alpha = 0.2, \beta = -1, \sigma = 3, \gamma = 0.05$ and $\delta = 0.55$.

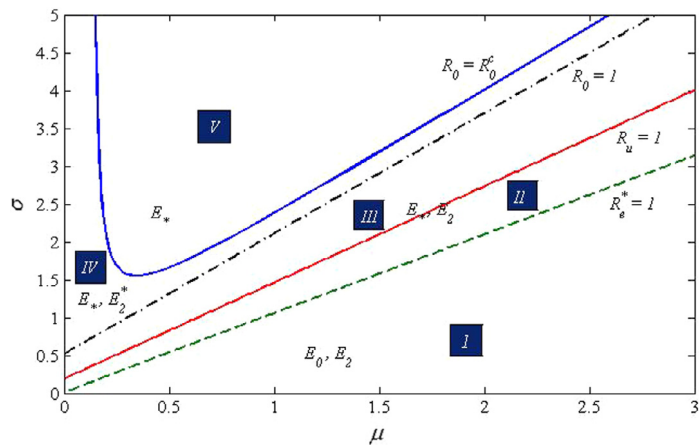


Fig. 5. Regions of model behavior in the two-parameter space (μ, σ) where σ is the transmission parameter and μ is the disease-induced death rate. In each region, stable equilibria are indicated. The regions marked I through IV are bistable, whereas the region V is monostable with eventual host extinction. Region IV can be endemic, while regions I and II can be disease-free. Host extinction is possible in all regions. The line enclosing region V is a saddle–node bifurcation curve obtained using MatCont, while the dashed and dash-dotted lines are transcritical bifurcation curves. Solid line between the dashed and dash-dotted lines marks the emergence of the unstable non-trivial equilibrium \mathcal{E}^* . Parameter values used are $k = 0.5, u = 0.2, \alpha = 0.2, \beta = -1, \gamma = 0.05$ and $\delta = 0.55$.

perturbation from the disease-free equilibrium can lead to a catastrophic extinction of the host population from high density in the presence of a strong Allee effect. On the other hand, the model of Hilker [23] suggests that an extinction occurs abruptly from a level of large population size due to a saddle–node bifurcation. In a similar note, the model

presented here shows that the synergistic effects of infectious disease and the strong Allee effect could lead to an inevitable crash of the host. Additionally, the bifurcation results reveal that the abrupt population collapse from a level of high population size varies from one species to another in relation to the strength of the impact of cooperative survival strategies on mortality rate function $D(N)$, which can be conveniently measured by the parameter β . In fact, the gradient of $D(N)$ at zero linearly depends on β and so, small value of the gradient or equivalently large value of β indicates strong impact. If $\beta > 0$ then $D(N)$ is decreasing, representing a strong impact of cooperative survival strategies. Hence, obligate cooperative species would be in this category. For $\beta \leq 0$, however, $D(N)$ increases slowly reflecting a less impact of such strategies. Non obligate cooperative species would belong to this category. This follows from the fact that some species are more vulnerable to extinction than others [8]. Therefore, the parameter β makes the proposed model more general and biologically relevant. More precisely, the demographic rate functions of the model in [23] are special cases of those considered in this paper for $\beta = -1/ku$ when the parameter $\alpha = 0$. Identifying which species are more vulnerable than others to population decline and extinction plays a relevant role in conservation biology for guiding management actions. Simply because such an information would allow biologists to improve the species' chances of survival.

The Allee effect and infectious disease are some of the extinction drivers that recently received considerable attention in the extinction research. Indeed, their joint interplay has long been recognized to drive host population to extinction. In particular, their synergistic effects define a tipping point at which the population crashes abruptly. The tipping point marking the unexpected population collapse is mathematically associated with a saddle–node bifurcation. When the two endemic equilibria \mathcal{E}_1^* and \mathcal{E}_2^* coalesce and disappear, there is no endemic attractor left and extinction is an eventual outcome. The endemic state \mathcal{E}_2^* emerges from the carrying capacity state if $\mathcal{R}_0 > 1$, which has a larger population size than \mathcal{E}_1^* . While the equilibrium \mathcal{E}_1^* bifurcates from the Allee threshold state on the disease-free boundary into the interior of the domain if $\mathcal{R}_u > 1$ or equivalently $\mathcal{R}_0 > \mathcal{R}_0^u$. The emergence of the unstable equilibrium \mathcal{E}_1^* establishes the extinction basin above the Allee threshold and it is essential for the saddle–node bifurcation to occur.

From biological point of view, the underlying mechanisms of the spontaneous population collapse are: the regulatory potential of the disease, which leads to a depression of the host population size p_2^* at endemic equilibrium and additional disease induced mortality that increases the likelihood of extinction (i.e. the effective extinction threshold becomes larger). Therefore, the infection attacks the host from two ends of the population size spectrum, thereby reducing the range of possible endemic persistence. Hence extinction takes place when the range of viable population sizes could not exist. Finally, the endemic population equilibrium is absorbed by the extinction basin, which is established by the disease.

It is well known that highly pathogenic species cause their own extinction but not that of their host [1,2]. As a consequence, a second saddle–node bifurcation exists when varying disease pathogenicity. Unlike in the case of forward hysteresis [17,19], the two saddle–node bifurcations are separate from each other when they exist. In this case, control measures by impacting the basic reproduction number can be either beneficial or disadvantageous for the host. On one hand, increasing \mathcal{R}_0 can be beneficial if it is altered above \mathcal{R}_0^{c2} , because it facilitates host endemic persistence rather extinction. On the other hand, decreasing \mathcal{R}_0 can be detrimental if it is reduced below \mathcal{R}_0^{c2} as it can drive host population to extinction.

In conclusion, the main differences between the model presented here and that introduced by Hilker in [23] are the inclusion of the exposed class and incorporating the more general quadratic rate functions which effectively capture species' susceptibility variation due to the Allee effects.

Acknowledgments

The support of South African DST/NRF SARChI chair on Mathematical Models and Methods in Bioengineering and Biosciences (N00317) is acknowledged, with gratitude. The authors acknowledge the support of the NC State/University of Pretoria collaborative agreement. The corresponding author acknowledges the support of Tertiary Education Trust Fund of Nigeria. The authors thank the anonymous reviewers and the handling editor for their constructive comments, suggestions and valuable corrections which have enhanced the paper.

Appendix A. Bifurcation diagrams for varying the parameter β

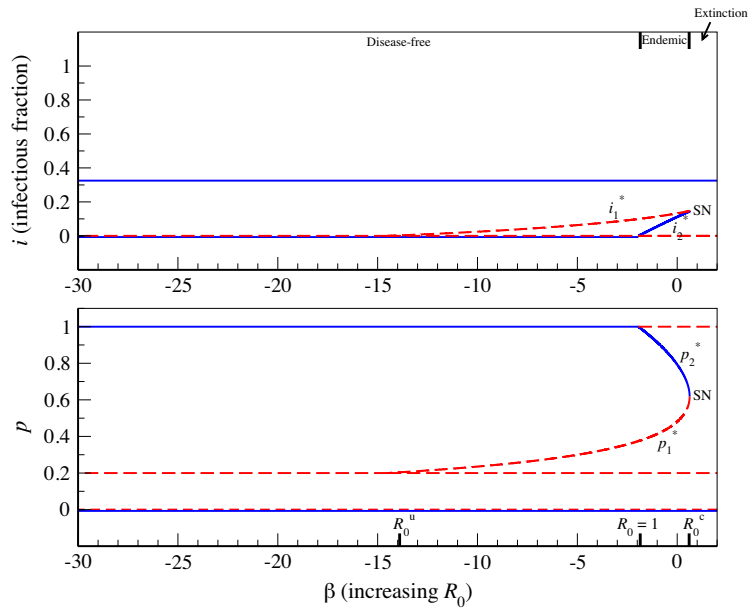


Fig. 6. Bifurcation diagrams for varying the parameter β (increasing \mathcal{R}_0), showing the biologically feasible equilibria. Solid (dashed) lines represent stable (unstable) equilibria and SN indicates a saddle–node bifurcation above which the population collapse. Parameter values used are $k = 0.5$, $u = 0.2$, $\mu = 0.55$, $\alpha = 0.2$, $\gamma = 0.05$, $\delta = 0.2$ and $\sigma = 3$.

Appendix B. The limit point curve in (β, δ) -space

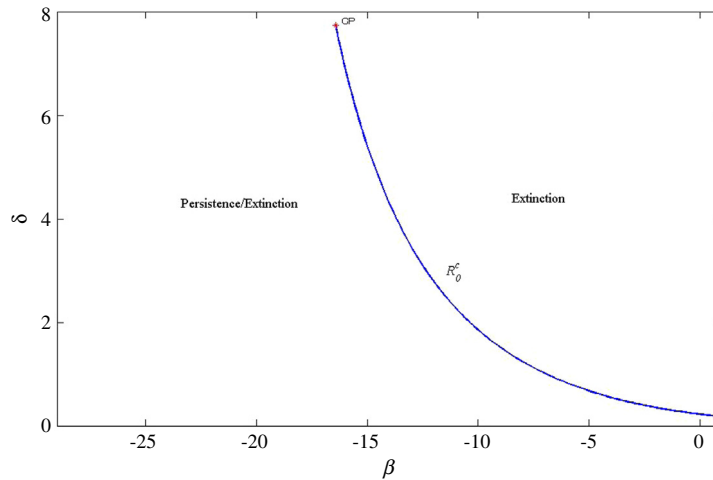


Fig. 7. The limit point curve in two parameter space (β, δ) showing the extinction risk at high population levels. Parameter values used are $k = 0.5$, $u = 0.2$, $\mu = 0.55$, $\alpha = 0.2$, $\gamma = 0.05$, and $\sigma = 3$.

References

[1] R.M. Anderson, Parasite pathogenicity and the depression of host population equilibria, *Nature* 279 (1979) 150–152.
 [2] R.M. Anderson, R.M. May, Population biology of infectious diseases: Part I, *Nature* 280 (1979) 361–367.

- [3] L. Berec, E. Angulo, F. Courchamp, Multiple Allee effect and population management, *Trends Ecol. Evol.* 22 (2007) 185–191.
- [4] B. Buonoma, D. Licitignola, On the backward bifurcation of a vaccination model with nonlinear incidence, *Nonlinear Anal. Model. Control* 16 (1) (2011) 30–46.
- [5] S. Busenberg, K.L. Cooke, H. Thieme, Demographic change and persistence of HIV/AIDS in a heterogeneous population, *SIAM J. Appl. Math.* 51 (4) (1991) 1030–1052.
- [6] S. Busenberg, P. Van den Driessche, Analysis of a disease transmission model in a population with varying size, *J. Math. Biol.* 28 (1990) 257–270.
- [7] L. Cai, G. Chen, D. Xiao, Multiparametric bifurcations of an epidemiological model with strong Allee effect, *J. Math. Biol.* 67 (2) (2013) 185–215.
- [8] B. Carmen, L. Stephane, C. Jean, Allee effects, mating systems and the extinction risk in populations with two sexes, *Ecol. Lett.* 7 (9) (2004) 802–812.
- [9] F. Courchamp, T. Clutton-Brock, B. Grenfell, Inverse density dependence and the Allee effect, *Trends Ecol. Evol.* 14 (1999) 405–410.
- [10] F. Courchamp, D. Mackdonald, Crucial importance of pack size in African wild dog, *Lycoan pictus*, *Anim. Conserv.* 4 (2001) 169–174.
- [11] S.B. David, B. Ludek, Single-species models of the Allee effect: extinction boundaries, sex ratios and mate encounters, *J. Theoret. Biol.* 218 (2002) 375–394.
- [12] A. Dhooge, W. Govaerts, Y.A. Kuznetsov, MatCont: A Matlab package for numerical bifurcation analysis of ODEs, *ACM Trans. Math. Software* 29 (2003) 141–164.
- [13] A. Friedman, A.-A. Yakubu, Fatal disease and demographic Allee effect: population persistence and extinction, *J. Biol. Dyn.* 6 (2) (2012) 495–508.
- [14] S.M. Garba, M.A. Safi, A.B. Gumel, Cross-immunity-induced backward bifurcation for a model of transmission dynamics of two strains of influenza, *Nonlinear Anal. RWA* 14 (2013) 1384–1403.
- [15] J. Gascoigne, R.N. Lipcius, Allee effect driven by predation, *J. Appl. Ecol.* 41 (2004) 801–810.
- [16] D. Greenhalgh, O. Diekmann, M.C.M. de Jong, Subcritical endemic steady states in mathematical models for animal infections with incomplete immunity, *Math. Biosci.* 165 (2000) 1–25.
- [17] D. Greenhalgh, M. Griffiths, Backward bifurcation, equilibrium and stability of phenomenon in a three-stage extended BSRV epidemic model, *J. Math. Biol.* 59 (1) (2009) 1–36.
- [18] D. Greenhalgh, M. Griffiths, Dynamic phenomena arising from an extended core group model, *Math. Biosci.* 221 (2) (2009) 136–149.
- [19] H. Gulbudak, M. Martcheva, Forward hysteresis and backward bifurcation caused by culling in an avian influenza model, *Math. Biosci.* 246 (1) (2013) 202–212.
- [20] A.B. Gumel, Causes of backward bifurcation in some epidemiological models, *J. Math. Anal. Appl.* 395 (2012) 355–365.
- [21] K.P. Hadeler, P. van den Driessche, Backward bifurcation in epidemic control, *Math. Biosci.* 146 (1) (1997) 15–35.
- [22] H.W. Hethcote, The mathematics of infectious diseases, *SIAM Rev.* 42 (2000) 599–653.
- [23] F.M. Hilker, Population collapse to extinction: the catastrophic combination of parasitism and Allee effect, *J. Biol. Dyn.* 4 (1) (2010) 86–101.
- [24] F.M. Hilker, M. Langlias, H. Malchow, The Allee effect and infectious diseases: Extinction, multiplicity, and the (dis-)appearance of oscillations, *Am. Nat.* 173 (2009) 72–88.
- [25] D.H. Knipl, G. Röst, Backward bifurcation in SIVS model with immigration of non-infectives, *Biomath* 2 (2013) 1312051. <http://dx.doi.org/10.111145/j.biomath.2013.12.051>.
- [26] C.C. McCluskey, J. Arino, P. van den Driessche, Global results for an epidemic model with vaccination that exhibits backward bifurcation, *SIAM J. Appl. Math.* 64 (1) (2003) 260–276.
- [27] M. Safan, H. Heesterbeek, K. Dietz, The minimum effort required to eradicate infections in models with backward bifurcation, *J. Math. Biol.* 53 (4) (2006) 703–718.
- [28] M.A. Safi, A.B. Gumel, Mathematical analysis of a disease transmission model with quarantine, isolation and an imperfect vaccine, *Comput. Math. Appl.* 61 (2011) 3044–3070.
- [29] D.A. Sánchez, *Ordinary Differential Equations and Stability Theory: An introduction*, Courier Dover Publications, 1979.
- [30] A.M. Stuart, A.R. Humphries, *Dynamical Systems and Numerical Analysis*, Cambridge University Press, 1998.
- [31] H.R. Thieme, T. Dhirasakdanon, Z. Han, R. Trevino, Species decline and extinction: synergy of infectious diseases and Allee effect? *J. Biol. Dyn.* 3 (2–3) (2009) 305–323.
- [32] S. Usaini, R. Anguelov, S.M. Garba, Dynamics of SI epidemic with a demographic Allee effect, *Theor. Popul. Biol.* 106 (2015) 113. <http://dx.doi.org/10.1016/j.tpb.2015.10.005>.